Neural-Network-Based Adaptive Fixed-Time Control for a 2-DOF Helicopter System With Input Quantization and Output Constraints

Zhijia Zhao, *Member, IEEE*, Jiale Wu, Chaoxu Mu, *Senior Member, IEEE*, Yu Liu, *Senior Member, IEEE*, and Keum-Shik Hong, *Fellow, IEEE*

***Abstract*— This study proposes a neural-network (NN)-based adaptive fixed-time control method for a two-degree-of-freedom (2-DOF) nonlinear helicopter system with input quantization and output constraints. First, a hysteresis quantizer is employed to mitigate chattering during signal quantization, and adaptive variables are utilized to eliminate errors in the quantization process. Subsequently, the system uncertainties are approximated using a radial basis function NN. Simultaneously, a logarithmic barrier Lyapunov function (BLF) is constructed to prevent the system outputs from violating the constraint boundaries. Based on a rigorous Lyapunov stability analysis and the fixed-time stability criterion, the signals of the closed-loop system are proven to be bounded within a fixed time. Finally, numerical simulations and experiments verified the feasibility of the proposed method.**

***Index Terms*— Adaptive neural-network (NN) control, fixed-time, input quantization, output constraints, two-degree-of-freedom (2-DOF) helicopter.**

I. Introduction

IN RECENT years, there has been a growing interest in unmanned aerial vehicles due to advancements in automation, information technology, and unmanned vehicles in general. In particular, unmanned helicopters are widely utilized in various fields because of their small size, high reliability, and hovering capabilities [1]. For example, they are employed in civil applications such as environmental monitoring [2], aerial surveying and mapping [3], disaster relief, and power patrols. In the military domain, unmanned helicopters are used for target reconnaissance and ground attacks [4]. However, helicopters are nonlinear systems with interaxis cross-coupling and complex dynamics, which pose significant challenges in controller design. Therefore, developing high-performance flight controllers is necessary to ensure the robustness of helicopter systems.

To address stability issues in unmanned helicopter control systems, various control methods have been developed. For example, Raghappriya and Kanthalakshmi [5] developed a sliding mode control algorithm to deal with fault issues for helicopter systems and validated the stability of their method through simulations. In [6], a simplified robust controller was introduced to suppress disturbances and ensure improved tracking performance. Sadala et al. [7] devised a novel sliding mode control to reduce error oscillations and stabilize system tracking. The aforementioned studies relied on known system models. However, in practical applications, helicopter systems often possess uncertain model parameters. Consequently, when designing control strategies for helicopter systems, comprehensively accounting for system uncertainty is crucial to accurately reflect the actual operating conditions.

In estimating system uncertainties, neural networks (NNs) play a significant role owing to their remarkable learning and nonlinear mapping capabilities [8], [9]. Moreover, the real-time decision-making ability of NNs enables helicopters to better adapt to complex and changing flight environments. In recent years, an increasing number of researchers have applied NNs to helicopter systems. For example, Chen et al. [10] designed an NN fault-tolerant control strategy to address the unknown external disturbances that helicopter systems encounter and to compensate for actuator faults and input saturation. In [11], an RBFNN control algorithm with inverse compensation was developed to enhance the stability performance via deterministic learning. A recursive NN control method was employed in [12] to handle uncertain dynamic models in the system, achieving intelligent formation control of unmanned helicopters. In [13], an NN-control-based approach was designed to constrain errors within a specified performance range. However, the aforementioned studies have primarily addressed unc ertainties for helicopters and other

Manuscript received 18 July 2023; revised 13 January 2024; accepted 9 May 2024. Date of publication 29 May 2024; date of current version 7 April 2025. This work was supported in part by the National Key Research and Development Program of China under Grant 2023YFB4706400; in part by the National Natural Science Foundation of China under Grant 62273112 and Grant 62333016; in part by the Guangdong Basic and Applied Basic Research Foundation under Grant 2023B1515120018 and Grant 2023B1515120019; in part by the Science and Technology Planning Project of Guangzhou, China, under Grant 2023A03J0120; in part by the National Research Foundation of Korea funded by the Ministry of Science and ICT, South Korea, under Grant IRIS-2023-00207954; and in part by the Guangzhou University Research Project under Grant RC2023037. *(Corresponding author: Zhijia Zhao.)*

Zhijia Zhao and Jiale Wu are with the School of Mechanical and Electrical Engineering, Guangzhou University, Guangzhou 510006, China (e-mail: zhjzhaoscut@163.com; 2112107005@e.gzhu.edu.cn).

Chaoxu Mu is with the School of Electrical and Information Engineering, Tianjin University, Tianjin 300072, China (e-mail: cxmu@tju.edu.cn).

Yu Liu is with the School of Automation Science and Engineering, South China University of Technology, Guangzhou 510640, China (e-mail: auylau@scut.edu.cn).

Keum-Shik Hong is with the Institute for Future, School of Automation, Qingdao University, Qingdao 266071, China, and also with the School of Mechanical Engineering, Pusan National University, Busan 46241, South Korea (e-mail: kshong@pusan.ac.kr).

Digital Object Identifier 10.1109/TNNLS.2024.3403145

systems, while ignoring the bandwidth limitation issue in networked control. This neglect can result in reduced signal transmission accuracy and impact the stability of the helicopter system. Quantizing the signals is a possible solution to this problem, and this motivates us to conduct further research.

Quantization is a common form of nonlinear input that reduces the communication burden and resource consumption by converting continuous signals into discrete forms [14]. This beneficial characteristic of quantization has garnered widespread interest. For example, Zhao et al. [15] introduced a hysteresis quantizer into the control input and employed an adaptive approach to estimate unknown parameters and compensate for quantization errors. Zhang et al. [16] designed an adaptive feedback control to achieve stable tracking of nonlinear systems with input quantization. Furthermore, Wang et al. [17] presented an adaptive backstepping control strategy that achieved joint control of input and state quantization in nonlinear systems. Although the aforementioned studies made considerable progress in input quantization for nonlinear systems, relatively few studies have addressed output constraints. In the realm of helicopters, the outputs of the system can be constrained by external environmental factors, which in turn can impact the stabilizing performance during flight.

In recent years, scholars have proposed various control methods to overcome the challenges posed by output constraints. For instance, Yu et al. [18] proposed a tangent-type barrier Lyapunov function (BLF) to solve the output constraint problem and stabilize the control of robot systems. In [19], a BLF was designed to effectively address the output constraints, and its effectiveness was verified on a helicopter experimental platform. Wu et al. [20] proposed a BLF to guarantee the constraints on vibration amplitude and prove the boundedness of the system errors. Although the aforementioned studies on output constraints for nonlinear systems have made significant progress, only a limited number of studies have focused on input quantization and output constraints for two-degree-of-freedom (2-DOF) helicopter systems. Furthermore, in practical applications, helicopter systems typically need to achieve fast and accurate responses within a finite time and remain stable thereafter.

Recently, the finite-time control has been increasingly utilized owing to its high control precision and fast convergence speed [21]. For example, Wei and Li [22] designed a new adaptive NN control algorithm that utilized finite-time control to improve the steady-state performance of nonlinear systems. Li et al. [23] proposed an adaptive control strategy for robot manipulators to ensure stability within a finite time. However, the finite-time control relies on the initial value of the system, which implies that the settling time of the system will vary for different initial conditions. When the initial state cannot be determined in advance, it becomes impossible to accurately estimate the settling time of the system.

To overcome the above limitations, Polyakov first introduced the fixed-time stability theory in [24]. This theory not only eliminates the dependence of convergence time on initial conditions but also achieves faster settling rates, which instead depend only on the control design parameters. This characteristic has been widely utilized. For example, in [25], a fixed-time stability control was developed to guarantee the fast convergence of errors in flexible robot systems and resolve amplitude constraint issues. In [26], the impact of input quantization and external disturbances on the system was addressed, and convergence stability of errors in multimechanical systems within a fixed time was achieved. Furthermore, Zhang and Wu [27] designed an adaptive tracking control algorithm using a symmetric Lyapunov function to ensure that the system trajectory was stabilized within a fixed time. However, the aforementioned studies focused only on the individual aspects of fixed-time stability control (e.g., quantization or constraints in nonlinear systems) without considering the potential interaction between quantization, constraints, and fixed-time control in practical applications. Therefore, extending fixed-time control to incorporate input quantization and output constraints in a 2-DOF nonlinear helicopter system is crucial.

Driven by the results and limitations of the aforementioned studies, we aim to investigate a fixed-time adaptive NN control method with input quantization and output constraints. The following are the primary contributions of this study.

1) Unlike the quantizer discussed in [26], this study utilizes a hysteresis quantizer that provides additional quantization levels to mitigate chattering effects. Furthermore, a logarithmic BLF is employed to constrain the output amplitude of the system.
2) Compared with finite-time control in [22] and [28], the convergence time of the proposed control method is determined by the design parameters and is not affected by the initial state, thereby further improving the transient system performance.
3) This study integrates input quantization and output constraints within a fixed-time framework and proposes an adaptive NN control scheme. The validity of the proposed method is demonstrated through theoretical analysis and experimental validation.

The remaining chapters of this article are organized as follows. Section II presents the problem formulation and a preliminary study. Section III explains the design of the fixed-time adaptive NN control and analyzes its stability. Section IV describes the numerical simulation results. In Section V, comparative experiments are conducted to analyze the feasibility of the proposed control. Finally, Section VI presents the conclusion of this study.

II. Problem Statement and Preliminary Study

A. Problem Statement

Fig. 1 illustrates a simplified diagram of a 2-DOF helicopter. The helicopter is equipped with two propellers. The horizontally positioned propeller generates a force denoted by F_p, which is located at a distance r_p from the center of the helicopter, and it controls the pitch motion. The vertically positioned propeller generates a force denoted as F_y, which is located at a distance r_y from the center of the helicopter, and it controls the yaw motion.

The Lagrangian mechanics approach is employed to model the 2-DOF helicopter system, and its dynamic system model

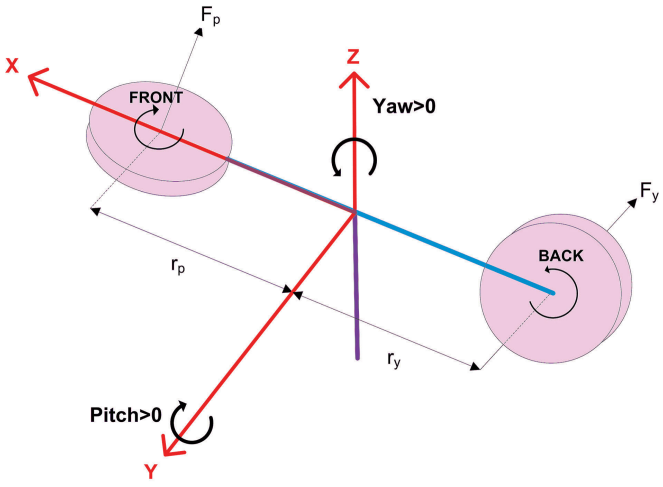

Fig. 1. Simplified sketch of a 2-DOF helicopter.

is described as [29]

$$\left(J_f + m_a l_v^2\right)\ddot{\theta} = K_{pp}V_f + K_{py}V_d - m_a g l_v \cos(\theta) - D_f\dot{\theta} - m_a l_v^2 \dot{\psi}^2 \sin(\theta)\cos(\theta) \tag{1}$$

$$\left(J_d + m_a l_v^2 \cos^2(\theta)\right)\ddot{\psi} = K_{yp}V_f + K_{yy}V_d - D_d\dot{\psi} + 2m_a l_v^2 \dot{\psi}\dot{\theta}\sin(\theta)\cos(\theta) \tag{2}$$

where m_a is the mass; g is the acceleration due to gravity; θ and ψ are the pitch and yaw angles, respectively; l_v is the distance from the center of mass to the pivot; K_{pp}, K_{py}, K_{yp}, and K_{yy} are the thrust torque constants; D_f and D_d are the friction coefficients; and J_f and J_d are the moments of inertia pertaining to the pitch and yaw axes, respectively.

We define $q = [q_1, q_2]^{\mathrm{T}}$, where $q_1 = [\theta, \psi]^{\mathrm{T}}$ and $q_2 = [\dot{\theta}, \dot{\psi}]^{\mathrm{T}}$. Considering the uncertainty and input quantization in the system, the dynamic equations of a 2-DOF helicopter can be translated into the following state-space model:

$$\dot{q}_1 = q_2 \tag{3}$$

$$\dot{q}_2 = G(q_1, q_2) + \Delta G(q_1, q_2) + \left(H(q_1, q_2) + \Delta H(q_1, q_2)\right) Q(u) \tag{4}$$

$$y = q_1 \tag{5}$$

where $\Delta G(q_1, q_2)$ and $\Delta H(q_1, q_2)$ are the system uncertainties, and $G(q_1, q_2)$ and $H(q_1, q_2)$ are given as follows:

$$G(q_1, q_2) = \begin{bmatrix} \dfrac{-m_a g l_v \cos(\theta) - D_f\dot{\theta} - m_a l_v^2 \dot{\psi}^2 \sin(\theta)\cos(\psi)}{J_f + m_a l_v^2} \\ \dfrac{-D_d\dot{\psi} + 2m_a l_v^2 \dot{\psi}\dot{\theta}\sin(\theta)\cos(\theta)}{J_d + m_a l_v^2 \cos^2(\theta)} \end{bmatrix} \tag{6}$$

$$H(q_1, q_2) = \begin{bmatrix} \dfrac{K_{pp}}{J_f + m_a l_v^2} & \dfrac{K_{py}}{J_f + m_a l_v^2} \\ \dfrac{K_{yp}}{J_d + m_a l_v^2 \cos^2(\theta)} & \dfrac{K_{yy}}{J_d + m_a l_v^2 \cos^2(\theta)} \end{bmatrix}. \tag{7}$$

Furthermore, y is the system output and u is the controller input. Unlike the logarithmic quantizer in [26], hysteresis quantizers are characterized by dwell time before a change in the system value, which can provide an additional level of quantization to eliminate chatter. Consequently, the following hysteresis quantizer is employed [30]:

$$Q(u(t)) = \begin{cases} u_k \mathrm{sgn}(u), & \dfrac{u_k}{1+\epsilon} < |u| < u_k,\ \dot{u} < 0, \text{ or} \\ & u_k < |u| \le \dfrac{u_k}{1-\epsilon},\ \dot{u} > 0 \\ u_k(1+\epsilon)\mathrm{sgn}(u), & u_k < |u| < \dfrac{u_k}{1-\epsilon},\ \dot{u} < 0, \text{ or} \\ & \dfrac{u_k}{1-\epsilon} < |u| \le \dfrac{u_k(1+\epsilon)}{(1-\epsilon)},\ \dot{u} > 0 \\ 0, & 0 \le |u| < \dfrac{u_{\min}}{1+\epsilon},\ \dot{u} < 0, \text{ or} \\ & \dfrac{u_{\min}}{1+\epsilon} \le u \le u_{\min},\ \dot{u} > 0 \\ Q\left(u\left(t^-\right)\right), & \dot{u} = 0 \end{cases} \tag{8}$$

where $u_k = \zeta^{1-\iota} u_{\min}$ with $\iota = 1, 2, \ldots$; $u_{\min} > 0$; $0 < \zeta < 1$; and $\epsilon = ((1-\zeta)/(1+\zeta))$. The quantized input $Q(u) = [V_f, V_d]^{\mathrm{T}}$ is in the set $\Omega = \{0, \pm u_k, \pm u_k(1+\epsilon)\}$. The parameter $u_{\min}$ determines the size of the dead zone of the quantizer. To devise an effective control strategy, we partition the hysteresis quantizer into two distinct parts described as [31]

$$Q(u(t)) = u + \varpi(t) \tag{9}$$

where u denotes the linear part, $\varpi(t)$ is the nonlinear part, and $\varpi(t) = Q(u(t)) - u \in \mathbb{R}^{2\times 1}$.

Substituting (9) into (4) yields

$$\begin{aligned} \dot{q}_2 &= G(q_1, q_2) + \Delta G(q_1, q_2) + H(q_1, q_2)u + H(q_1, q_2)\varpi(t) \\ &\quad + \Delta H(q_1, q_2)(u + \varpi(t)) \\ &= G(q_1, q_2) + H(q_1, q_2)u + P(q, u) + H(q_1, q_2)\varpi(t) \end{aligned} \tag{10}$$

where $P(q, u) = \Delta G(q_1, q_2) + \Delta H(q_1, q_2)(u + \varpi(t))$.

Lemma 1 [22]: The nonlinear part $\varpi(t)$ satisfies the following inequalities:

$$\varpi^2(t) \le \epsilon^2 u^2 \quad \forall |u| \ge u_{\min} \tag{11}$$

$$\varpi^2(t) \le u_{\min}^2 \quad \forall |u| \le u_{\min}. \tag{12}$$

Assumption 1 [32]: For the control gain function $H(q_1, q_2)$, there exist unknown positive constants H_m and H_M such that $0 < H_m < |H(q_1, q_2)| < H_M$.

Assumption 2 [33]: The desired trajectory q_d is a continuously differentiable function, and q_d, $\dot{q}_d$, and $\ddot{q}_d$ are bounded.

Lemma 2 [34]: Suppose that there exists a constant $c_t > 0$. Then, for any $z \in \mathbb{R}$ with $|z| < |c_t|$, the following inequality

holds:

$$\ln\frac{c_t^2}{c_t^2 - z_1^{\mathrm{T}} z_1} \leq \frac{z_1^{\mathrm{T}} z_1}{c_t^2 - z_1^{\mathrm{T}} z_1}. \tag{13}$$

Lemma 3 [35]: For any real number a and positive constant f, the following inequality is obtained:

$$0 \leq |a| - a\tanh\left(\frac{a}{f}\right) \leq 0.2785 f. \tag{14}$$

B. NN Approximation

The RBFNN has become increasingly popular for its exceptional ability to accurately estimate unknown nonlinear functions. In this study, we employ the following RBFNN to estimate a continuous function $h_n(Z): \mathbb{R}^l \to \mathbb{R}$:

$$h_n(Z) = \Theta^{\mathrm{T}} \Phi(Z) \tag{15}$$

where $Z \in \mathbb{R}^l$ is the input vector, and $\Theta = [\theta_1, \theta_2, \ldots, \theta_i]^{\mathrm{T}} \in \mathbb{R}^i$ is the weight vector, with $i > 1$ being the number of neurons. In addition, $\Phi(Z) = [\Phi_1(Z), \Phi_2(Z), \ldots, \Phi_i(Z)]^{\mathrm{T}}$ is a Gaussian function vector, represented by $\Phi_j(Z) = \exp(-(Z-\delta_j)^{\mathrm{T}}(Z-\delta_j)/\Upsilon_j^2)$, where $\delta_j = [\delta_{j1}, \delta_{j2}, \ldots, \delta_{jl}]^{\mathrm{T}}$ and Υ_j are the center and width of the basis function, respectively.

By selecting a sufficient number of neurons, the RBFNN can smoothly estimate an arbitrary continuous function in the compact set $\Omega_z \in \mathbb{R}^l$ to any desired accuracy as

$$h(Z) = \Theta^{*\mathrm{T}} \Phi(Z) + \eta(Z) \tag{16}$$

where Θ^* is the optimal weight vector, and $\eta(Z)$ is the approximation error that satisfies $\|\eta(Z)\| \leq \bar{\eta}$ with $\bar{\eta} > 0$. The ideal weight vector Θ^* can be expressed as

$$\Theta^* = \arg\min_{\Theta \in R^i} \left\{ \sup_{Z \in \Omega_z} \left| h(Z) - \Theta^{\mathrm{T}} \Phi(Z) \right| \right\}. \tag{17}$$

Remark 1: The structure of the RBFNN, as shown in Fig. 2, typically consists of three layers: the input, hidden, and output layers [36]. In the input layer, each node represents a feature or variable from the input data. This input data is received by the input layer and transmitted to the hidden layer. Within the hidden layer, neurons employ radial basis functions to transform and extract features from the input data. Subsequently, the output layer receives information from the hidden layer and generates the final output of the network.

C. Fixed-Time

Consider a nonlinear system

$$\dot{x}(t) = f(x(t)), \quad x(0) = x_0 \tag{18}$$

where $x \in R^n$ and $f: \mathbb{R}^+ \times \mathbb{R}^n \to \mathbb{R}^n$ are the system variables and nonlinear function, respectively. For system (18), the origin is assumed to act as an equilibrium point.

Definition 1 [37]: The origin of the system (18) is finite-time stable if it is globally asymptotically stable and there exists a convergence time function $\mathrm{T}: \mathbb{R}^n \to \mathbb{R}^+$ such that for any $x_0 \in \mathbb{R}^n$, the solution $x(t, x_0)$ of system (18) is defined and $x(t, x_0) \in \mathbb{R}^n$ for $t \in [0, \mathrm{T}(x_0))$ and $\lim_{t \to \mathrm{T}(x_0)} x(t, x_0) = 0$ hold.

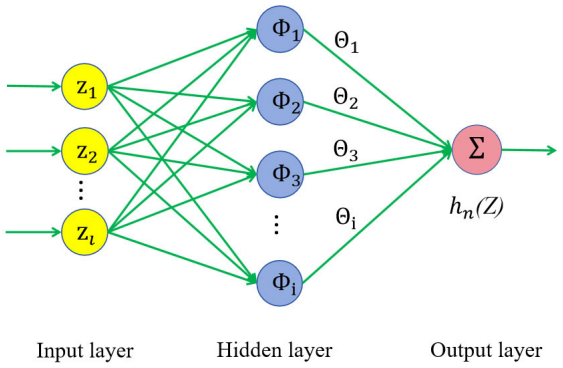

Fig. 2. Structure of the RBFNN.

TABLE I
STABLE CONDITION AND CONVERGENCE TIME FOR FINITE-TIME AND FIXED-TIME

Control method	Stable condition	Convergence time
Finite − time	$\dot{V}(x) \leq -\mu_2 V^{\gamma}(x)$	$T \leq T_{\max} = \frac{1}{\mu_2(1-\gamma)} V(x(0))^{1-\gamma}$
Fixed − time	$\dot{V}(x) \leq -\mu_1 V^{\beta}(x) - \mu_2 V^{\gamma}(x)$	$T \leq T_{\max} = \frac{1}{\mu_1(\beta-1)} + \frac{1}{\mu_2(1-\gamma)}$

Definition 2 [37]: The origin of the system (18) is fixed-time stable if it is globally finite-time stable and for any $x(0)$, the settling time function $\mathrm{T}(x_0)$ is bounded. That is, $\mathrm{T}(x(0)) < \mathrm{T}_{\max}$ for a constant $\mathrm{T}_{\max} > 0$.

Lemma 4 [38]: For a positive definite function $V(x)$, if there exist $\zeta_1 > 0$, $\zeta_2 > 0$, $\beta > 1$, and $0 < \gamma < 1$ satisfy the following:

$$\dot{V}(x) \leq -\zeta_1 V^{\beta}(x) - \zeta_2 V^{\gamma}(x) \tag{19}$$

then the origin of the system (18) is fixed-time stable. To estimate the convergence time, we use the following approximation:

$$\mathrm{T} \leq \mathrm{T}_{\max} = \frac{1}{\zeta_1(\beta-1)} + \frac{1}{\zeta_2(1-\gamma)}. \tag{20}$$

Remark 2: Table I lists the stability conditions and convergence times for finite-time and fixed-time. The convergence time of finite-time control depends on the initial value $V(x(0))$. Compared with finite-time control, the convergence time of fixed-time control is determined solely by the design parameters and is not affected by the initial states.

Lemma 5 [39]: For $c_1, c_2, \ldots, c_n \in \mathbb{R}$, and $0 \leq d \leq 1$, the following can be obtained:

$$(|c_1| + |c_2| + \cdots + |c_n|)^d \leq |c_1|^d + |c_2|^d + \cdots + |c_n|^d. \tag{21}$$

Lemma 6 [40]: If $L_m > 0$, $m = 1, 2, \ldots, n$, it can be derived that

$$\left(\sum_{m=1}^{n} L_m\right)^2 \leq n \cdot \sum_{m=1}^{n} L_m^2. \tag{22}$$

Lemma 7 [41]: For any real numbers b and d, the following can be obtained:

$$bd \leq \frac{\xi^{\varkappa}}{\varkappa}|b|^{\varkappa} + \frac{1}{\kappa \xi^{\kappa}}|d|^{\kappa} \tag{23}$$

where $\xi > 0$, $\varkappa > 1$, $\kappa > 1$, and $(\varkappa - 1)(\kappa - 1) = 1$.

III. NN Control Design

We define the tracking error variables as

$$z_1 = q_1 - q_d \tag{24}$$

$$z_2 = q_2 - \alpha \tag{25}$$

where $q_d = [\theta_d, \psi_d]^{\mathrm{T}}$ is the desired trajectory. Substituting (3) and (25) into the time derivative of z_1 yields

$$\dot{z}_1 = z_2 + \alpha - \dot{q}_d \tag{26}$$

where α is the virtual variable to be designed.

To satisfy the output constraint condition, we design the BLF candidate as

$$V_1 = \frac{1}{2}\ln\left(\frac{c_t^2}{c_t^2 - z_1^{\mathrm{T}} z_1}\right) \tag{27}$$

where $c_t > 0$ is a continuous function that constrains the amplitude of the error, and c_t is expressed as

$$c_t = ke^{-\varrho t} + h \tag{28}$$

where ϱ, k, and $h \geq 0$ are the design parameters.

Differentiating V_1 yields

$$\begin{aligned}\dot{V}_1 &= \frac{z_1^{\mathrm{T}}\dot{z}_1 - \frac{\dot{c}_t}{c_t} z_1^{\mathrm{T}} z_1}{c_t^2 - z_1^{\mathrm{T}} z_1} \\ &= \frac{z_1^{\mathrm{T}}(z_2 + \alpha - \dot{q}_d) - \frac{\dot{c}_t}{c_t} z_1^{\mathrm{T}} z_1}{c_t^2 - z_1^{\mathrm{T}} z_1}.\end{aligned} \tag{29}$$

The virtual variable α is designed as follows:

$$\begin{aligned}\alpha = &-k_{11}\frac{z_1\left(c_t^2 - z_1^{\mathrm{T}} z_1\right)}{z_1^{\mathrm{T}} z_1}\left(\frac{1}{2}\ln\left(\frac{c_t^2}{c_t^2 - z_1^{\mathrm{T}} z_1}\right)\right)^{\frac{1}{2}} \\ &- k_{12}\frac{z_1\left(c_t^2 - z_1^{\mathrm{T}} z_1\right)}{z_1^{\mathrm{T}} z_1}\left(\frac{1}{2}\ln\left(\frac{c_t^2}{c_t^2 - z_1^{\mathrm{T}} z_1}\right)\right)^{2} \\ &+ \dot{q}_d - \left(\frac{1}{2} + \varrho\right) z_1\end{aligned} \tag{30}$$

where k_{11} and k_{12} are positive constants.

Remark 3: The function $z_1/(z_1^{\mathrm{T}} z_1)$ in (30) results in chattering. To address this issue, a smoother approximation of the function is required. Using [25] as inspiration, we suggest the following method: when $z_1^{\mathrm{T}} z_1 < \nu_1$ with $\nu_1 > 0$ holds, $z_1^{\mathrm{T}} z_1$ is substituted with ν_1. The value of ν_1 can be initially set to a conservative value and then fine-tuned based on feedback from the system.

Considering $z_1^{\mathrm{T}} z_2 \leq (1/2) z_1^{\mathrm{T}} z_1 + (1/2) z_2^{\mathrm{T}} z_2$ and $|(\dot{c}_t/c_t)| \leq \varrho$, the substitution of (30) into (29) results in

$$\begin{aligned}\dot{V}_1 \leq &\frac{\frac{1}{2} z_2^{\mathrm{T}} z_2}{c_t^2 - z_1^{\mathrm{T}} z_1} - k_{11}\left(\frac{1}{2}\ln\left(\frac{c_t^2}{c_t^2 - z_1^{\mathrm{T}} z_1}\right)\right)^{\frac{1}{2}} \\ &- k_{12}\left(\frac{1}{2}\ln\left(\frac{c_t^2}{c_t^2 - z_1^{\mathrm{T}} z_1}\right)\right)^{2}.\end{aligned} \tag{31}$$

Since $P(q, u)$ in (10) is an unknown nonlinear function, it can be approximated by an RBFNN as follows:

$$P(q, u) = \Theta^{*\mathrm{T}}\Phi(Z) + \eta(Z) \tag{32}$$

where Θ^* and $\Phi(Z)$ are the ideal weight vector and basis function, respectively; $Z = [q_1^{\mathrm{T}}, q_2^{\mathrm{T}}, q_d^{\mathrm{T}}, \dot{q}_d^{\mathrm{T}}]^{\mathrm{T}}$ is the activation signal; and $\eta(Z)$ is an approximate error satisfying $\|\eta(Z)\| \leq \bar{\eta}$, where $\bar{\eta} > 0$ is a constant.

Hence, (10) can be rewritten as

$$\dot{q}_2 = G + Hu + \Theta^{*\mathrm{T}}\Phi(Z) + \eta(Z) + \delta \tag{33}$$

where $\delta = H(q_1, q_2)\varpi(t)$. Based on Lemma 1 and Assumption 2, we can derive that δ is bounded. Therefore, there exists an unknown positive constant $\bar{\delta}$ that satisfies $\|\delta\| \leq \bar{\delta}$. Moreover, we define $\tilde{\bar{\delta}} = \hat{\bar{\delta}} - \bar{\delta}$.

According to (25) and (33), the derivative of z_2 is derived as follows:

$$\begin{aligned}\dot{z}_2 &= \dot{q}_2 - \dot{\alpha} \\ &= G + Hu + \Theta^{*\mathrm{T}}\Phi(Z) + \eta + \delta - \dot{\alpha}.\end{aligned} \tag{34}$$

We select the following Lyapunov function:

$$V_2 = V_1 + \frac{1}{2} z_2^{\mathrm{T}} z_2. \tag{35}$$

Based on (34), the derivative of V_2 gives

$$\begin{aligned}\dot{V}_2 &= \dot{V}_1 + z_2^{\mathrm{T}}\dot{z}_2 \\ &= \dot{V}_1 + z_2^{\mathrm{T}}\left(G + Hu + \Theta^{*\mathrm{T}}\Phi(Z) + \eta + \delta - \dot{\alpha}\right).\end{aligned} \tag{36}$$

We propose the control law as

$$\begin{aligned}u = H^{-1}\Bigg(&-G - \frac{\frac{1}{2} z_2}{c_t^2 - z_1^{\mathrm{T}} z_1} - \hat{\Theta}^{\mathrm{T}}\Phi(Z) + \dot{\alpha} - \tanh\left(\frac{z_2}{\rho}\right)\hat{\bar{\delta}} \\ &- \frac{1}{2} z_2 - k_{21}\frac{z_2}{z_2^{\mathrm{T}} z_2}\left(\frac{1}{2} z_2^{\mathrm{T}} z_2\right)^{\frac{1}{2}} - k_{22}\left(\frac{1}{2}\right)^{2} z_2 z_2^{\mathrm{T}} z_2\Bigg)\end{aligned} \tag{37}$$

where k_{21} and k_{22} are positive constants.

The adaptive laws for $\hat{\Theta}$ and $\hat{\bar{\delta}}$ are devised as

$$\dot{\hat{\Theta}} = \Gamma_\Theta\left[\Phi(Z) z_2^{\mathrm{T}} - \hat{\Theta}\hat{\Theta}^{\mathrm{T}}\hat{\Theta} - \sigma_\Theta\hat{\Theta}\right] \tag{38}$$

$$\dot{\hat{\bar{\delta}}} = \varphi_{\bar{\delta}}\left[z_2^{\mathrm{T}}\tanh\left(\frac{z_2}{\rho}\right) - \hat{\bar{\delta}}^3 - \sigma_{\bar{\delta}}\hat{\bar{\delta}}\right] \tag{39}$$

where $\Gamma_\Theta > 0$ and $\varphi_{\bar{\delta}} > 0$. Furthermore, σ_Θ and $\sigma_{\bar{\delta}}$ are small positive parameters.

Remark 4: Similar to Remark 3, the function $z_2/(z_2^{\mathrm{T}} z_2)$ in (37) causes chattering. To avoid this, the following approach is proposed: if the condition $z_2^{\mathrm{T}} z_2 < \nu_2$ holds, then the value of $z_2^{\mathrm{T}} z_2$ is replaced by ν_2, where ν_2 is a positive constant. The value ν_2 can be initially set to a small value and then improved based on feedback from the system.

Substituting (37) into (36) yields

$$\begin{aligned}\dot{V}_2 = &-k_{11}\left(\frac{1}{2}\ln\left(\frac{c_t^2}{c_t^2 - z_1^{\mathrm{T}}z_1}\right)\right)^{\frac{1}{2}} - k_{21}\left(\frac{1}{2}z_2^{\mathrm{T}}z_2\right)^{\frac{1}{2}} + z_2^{\mathrm{T}}\eta \\ &- k_{12}\left(\frac{1}{2}\ln\left(\frac{c_t^2}{c_t^2 - z_1^{\mathrm{T}}z_1}\right)\right)^{2} - k_{22}\left(\frac{1}{2}z_2^{\mathrm{T}}z_2\right)^{2} + z_2^{\mathrm{T}}\delta \\ &- z_2^{\mathrm{T}}\tilde{\Theta}^{\mathrm{T}}\Phi(Z) - \frac{1}{2}z_2^{\mathrm{T}}z_2 - z_2^{\mathrm{T}}\tanh\left(\frac{z_2}{\rho}\right)\hat{\bar{\delta}} \end{aligned} \tag{40}$$

where $\tilde{\Theta} = \hat{\Theta} - \Theta^*$. Considering the effect of $\tilde{\Theta}$ and $\tilde{\bar{\delta}}$ on system stability, the Lyapunov function candidate is designed as

$$V_3 = V_2 + \mathrm{tr}\left\{\frac{1}{2}\tilde{\Theta}^{\mathrm{T}}\Gamma_{\Theta}^{-1}\tilde{\Theta}\right\} + \frac{1}{2\varphi_{\bar{\delta}}}\tilde{\bar{\delta}}^2. \tag{41}$$

Its time derivative is expressed as

$$\begin{aligned}\dot{V}_3 &= \dot{V}_2 + \mathrm{tr}\left\{\tilde{\Theta}^{\mathrm{T}}\Gamma_{\Theta}^{-1}\dot{\hat{\Theta}}\right\} + \frac{1}{\varphi_{\bar{\delta}}}\tilde{\bar{\delta}}\dot{\hat{\bar{\delta}}} \\ &= -k_{11}\left(\frac{1}{2}\ln\left(\frac{c_t^2}{c_t^2 - z_1^{\mathrm{T}}z_1}\right)\right)^{\frac{1}{2}} - k_{21}\left(\frac{1}{2}z_2^{\mathrm{T}}z_2\right)^{\frac{1}{2}} + z_2^{\mathrm{T}}\eta \\ &\quad - k_{12}\left(\frac{1}{2}\ln\left(\frac{c_t^2}{c_t^2 - z_1^{\mathrm{T}}z_1}\right)\right)^{2} - k_{22}\left(\frac{1}{2}z_2^{\mathrm{T}}z_2\right)^{2} + z_2^{\mathrm{T}}\delta \\ &\quad - z_2^{\mathrm{T}}\tanh\left(\frac{z_2}{\rho}\right)\hat{\bar{\delta}} + \tilde{\bar{\delta}}z_2^{\mathrm{T}}\tanh\left(\frac{z_2}{\rho}\right) - \frac{1}{2}z_2^{\mathrm{T}}z_2 \\ &\quad - \sigma_{\Theta}\mathrm{tr}\left\{\tilde{\Theta}^{\mathrm{T}}\hat{\Theta}\right\} - \mathrm{tr}\left\{\tilde{\Theta}^{\mathrm{T}}\hat{\Theta}\hat{\Theta}^{\mathrm{T}}\hat{\Theta}\right\} - \sigma_{\bar{\delta}}\tilde{\bar{\delta}}\hat{\bar{\delta}} - \tilde{\bar{\delta}}\hat{\bar{\delta}}^3 \end{aligned} \tag{42}$$

where $z_2^{\mathrm{T}}\eta \le (1/2)z_2^{\mathrm{T}}z_2 + (1/2)\bar{\eta}^2$. From Lemma 7, we obtain

$$-\sigma_{\Theta}\mathrm{tr}\left\{\tilde{\Theta}^{\mathrm{T}}\hat{\Theta}\right\} \le -\sigma_{\Theta}\left(\tilde{\Theta}^{\mathrm{T}}\tilde{\Theta}\right)^{\frac{1}{2}} + \frac{\sigma_{\Theta}}{2}\left(\Theta^{*\mathrm{T}}\Theta^* + 1\right) \tag{43}$$

$$\begin{aligned}-\mathrm{tr}\left\{\tilde{\Theta}^{\mathrm{T}}\hat{\Theta}\hat{\Theta}^{\mathrm{T}}\hat{\Theta}\right\} &= -\left\|\tilde{\Theta}\right\|^4 - \left\|\Theta^*\right\|^2\left(\left\|\tilde{\Theta}\right\|^2 + \tilde{\Theta}^{\mathrm{T}}\Theta^*\right) \\ &\quad - 3\left\|\tilde{\Theta}\right\|^2\tilde{\Theta}^{\mathrm{T}}\Theta^* - 2\left\|\tilde{\Theta}^{\mathrm{T}}\Theta^*\right\|^2 \\ &\le -\left(1 - \frac{9}{4}\kappa_1^{\frac{4}{3}} - \frac{1}{4\kappa_2^4}\right)\left\|\tilde{\Theta}\right\|^4 + \left\|\Theta^*\right\|^2 \\ &\quad + \left(\frac{3}{4\kappa_1^4} + \frac{3}{4}\kappa_2^{\frac{4}{3}}\right)\left\|\Theta^*\right\|^4 \\ &\quad - 2\left\|\Theta^*\right\|^2\left(\tilde{\Theta}^{\mathrm{T}}\tilde{\Theta}\right)^{\frac{1}{2}} \end{aligned} \tag{44}$$

where $\kappa_1 > 0$ and $\kappa_2 > 0$. Furthermore, we use similar derivations for $\sigma_{\bar{\delta}}\tilde{\bar{\delta}}\hat{\bar{\delta}}$ and $\tilde{\bar{\delta}}\hat{\bar{\delta}}^3$.

Considering the inequalities as follows:

$$z_2^{\mathrm{T}}\delta \le \bar{\delta}\sum_{r=1}^{2}\left|z_{2r}\right| \tag{45}$$

$$z_2^{\mathrm{T}}\tanh\left(\frac{z_2}{\rho}\right) = \sum_{r=1}^{2}\left(z_{2r}\tanh\left(\frac{z_{2r}}{\rho}\right)\right). \tag{46}$$

Applying Lemma 3, we obtain

$$\sum_{r=1}^{2}\left|z_{2r}\right| - \sum_{r=1}^{2}\left(z_{2r}\tanh\left(\frac{z_{2r}}{\rho}\right)\right) \le 0.557\rho. \tag{47}$$

According to the inequalities (43), (44), and (47), then (42) can be rewritten as

$$\begin{aligned}\dot{V}_3 \le &-k_{11}\left(\frac{1}{2}\ln\left(\frac{c_t^2}{c_t^2 - z_1^{\mathrm{T}}z_1}\right)\right)^{\frac{1}{2}} - k_{21}\left(\frac{1}{2}z_2^{\mathrm{T}}z_2\right)^{\frac{1}{2}} \\ &- k_{12}\left(\frac{1}{2}\ln\left(\frac{c_t^2}{c_t^2 - z_1^{\mathrm{T}}z_1}\right)\right)^{2} - k_{22}\left(\frac{1}{2}z_2^{\mathrm{T}}z_2\right)^{2} \\ &- k_{13}\left(\tilde{\Theta}^{\mathrm{T}}\tilde{\Theta}\right)^{\frac{1}{2}} - k_{23}\left\|\tilde{\Theta}\right\|^4 - k_{14}\left(\tilde{\bar{\delta}}^2\right)^{\frac{1}{2}} - k_{24}\left\|\tilde{\bar{\delta}}\right\|^4 \\ &+ \left(\frac{3}{4\kappa_1^4} + \frac{3}{4}\kappa_2^{\frac{4}{3}}\right)\left\|\Theta^*\right\|^4 + \left(1 + \frac{\sigma_{\Theta}}{2}\right)\left\|\Theta^*\right\|^2 + \frac{\sigma_{\Theta}}{2} \\ &+ \left(\frac{3}{4\kappa_3^4} + \frac{3}{4}\kappa_4^{\frac{4}{3}}\right)\left\|\bar{\delta}\right\|^4 + \left(1 + \frac{\sigma_{\bar{\delta}}}{2}\right)\left\|\bar{\delta}\right\|^2 + \frac{\sigma_{\bar{\delta}}}{2} + \frac{1}{2}\bar{\eta} \end{aligned} \tag{48}$$

where $\kappa_3, \kappa_4 > 0$, k_{13}, k_{23}, k_{14}, and k_{24} are defined as

$$k_{13} = \min\left\{\frac{\sqrt{2}\left(2\left\|\Theta^*\right\|^2 + \sigma_{\Theta}\right)}{\sqrt{\lambda_{\max}\left(\Gamma_{\Theta}^{-1}\right)}}\right\} \tag{49}$$

$$k_{23} = \min\left\{\frac{4\left(1 - \frac{9}{4}\kappa_1^{\frac{4}{3}} - \frac{1}{4\kappa_2^4}\right)}{\left(\lambda_{\max}\left(\Gamma_{\Theta}^{-1}\right)\right)^2}\right\} \tag{50}$$

$$k_{14} = \min\left\{\frac{\sqrt{2}\left(2\left\|\bar{\delta}\right\|^2 + \sigma_{\bar{\delta}}\right)}{\sqrt{\left(\varphi_{\bar{\delta}}^{-1}\right)}}\right\} \tag{51}$$

$$k_{24} = \min\left\{\frac{4\left(1 - \frac{9}{4}\kappa_3^{\frac{4}{3}} - \frac{1}{4\kappa_4^4}\right)}{\left(\varphi_{\bar{\delta}}^{-1}\right)^2}\right\}. \tag{52}$$

Then, we can obtain

$$\dot{V}_3 \le -\mu_1 V_3^{\frac{1}{2}} - \frac{\mu_2}{4}V_3^2 + C \tag{53}$$

where

$$\mu_1 = \min\{k_{11}, k_{21}, k_{13}, k_{14}\} \tag{54}$$

$$\mu_2 = \min\{k_{12}, k_{22}, k_{23}, k_{24}\} \tag{55}$$

$$\begin{aligned}C = &\left(\frac{3}{4\kappa_1^4} + \frac{3}{4}\kappa_2^{\frac{4}{3}}\right)\left\|\Theta^*\right\|^4 + \left(1 + \frac{\sigma_{\Theta}}{2}\right)\left\|\Theta^*\right\|^2 + \frac{\sigma_{\Theta}}{2} \\ &+ \left(\frac{3}{4\kappa_3^4} + \frac{3}{4}\kappa_4^{\frac{4}{3}}\right)\left\|\bar{\delta}\right\|^4 + \left(1 + \frac{\sigma_{\bar{\delta}}}{2}\right)\left\|\bar{\delta}\right\|^2 + \frac{\sigma_{\bar{\delta}}}{2} + \frac{1}{2}\bar{\eta}. \end{aligned} \tag{56}$$

Theorem 1: Considering the 2-DOF helicopter system described by (3) and (4) with input quantization and output constraints, the fixed-time adaptive NN control law (37) and the updating laws (38) and (39) can be applied. Suppose the original state $(q(0), \dot{q}(0), \hat{\Theta}, \hat{\bar{\delta}})$ are bounded, then the closed-loop system signals z_1, z_2, $\tilde{\Theta}$, and $\tilde{\bar{\delta}}$ will converge into

compact sets Ω_{z_1}, Ω_{z_2}, $\Omega_{\tilde{\Theta}}$, and $\Omega_{\tilde{\bar{\delta}}}$ within a fixed time. The convergence time T can be approximated by

$$\mathrm{T} \leq \mathrm{T}_{\max} = \frac{2}{\mu_1} + \frac{4}{(1-\varepsilon)\,\mu_2} \tag{57}$$

where $0 < \varepsilon < 1$ is a constant, and the compact sets Ω_{z_1}, Ω_{z_2}, $\Omega_{\tilde{\Theta}}$, and $\Omega_{\tilde{\bar{\delta}}}$ are defined as

$$\Omega_{z_1} = \left\{ z_1 : \|z_1\| \leq \sqrt{c_t^2 \left(1 - \frac{1}{e^G}\right)} \right\} \tag{58}$$

$$\Omega_{z_2} = \left\{ z_2 : \|z_2\| \leq \sqrt{G} \right\} \tag{59}$$

$$\Omega_{\tilde{\Theta}} = \left\{ \tilde{\Theta} : \left\|\tilde{\Theta}\right\| \leq \sqrt{\frac{G}{\lambda_{\min}\left(\Gamma_\Theta^{-1}\right)}} \right\} \tag{60}$$

$$\Omega_{\tilde{\bar{\delta}}} = \left\{ \tilde{\bar{\delta}} : \left\|\tilde{\bar{\delta}}\right\| \leq \sqrt{\varphi_{\bar{\delta}} G} \right\} \tag{61}$$

where $G = 2((4C)/(\varepsilon\mu_2))^{1/2}$.

Remark 5: In recent fixed-time control methods [42], [43], the fixed-time stability analysis was performed by assuming the boundedness of the weight vector, which lacks a theoretical foundation. In this study, we design a new adaptive update law for the weight vector and rigorously demonstrate its boundedness through stability analysis.

IV. Numerical Simulation and Comparisons

This section describes two sets of MATLAB numerical simulations conducted to model the attitude tracking of helicopters. First, the proposed control is compared with the commonly used proportional differential (PD) control and the finite-time control in [44], verifying the feasibility of the proposed control. Subsequently, the tracking performances under different initial conditions are compared to verify the fixed-time stability of the proposed control method. The simulation parameters of the 2-DOF helicopter system are provided in Table II.

We define the continuous-time reference trajectory as the command for helicopter trajectory tracking. The desired trajectory is chosen as $q_d = [(\pi/18)\sin(t), (\pi/12)\sin(t)]^{\mathrm{T}}$, and the initial conditions of the helicopter are given as $q_1 = [0.01, 0.01]^{\mathrm{T}}$ and $q_2 = [0.01, 0.01]^{\mathrm{T}}$. The voltage supplied to the dc motor in the helicopter model is ± 24 V.

A. Comparison of the Proposed Control, PD Control, and the Finite-Time Control in [44]

1) Proposed Control: For the proposed NN-based adaptive fixed-time control, 64 nodes are used with centers uniformly distributed on $[-1, 1] \times [-1, 1] \times [-1, 1] \times [-1, 1] \times [-1, 1] \times [-1, 1] \times [-1, 1] \times [-1, 1]$. The initial weights are set as $\hat{\Theta}(0) = 0$, and the variance is set to 16. In addition, the control parameters are chosen as $k_{11} = 2$, $k_{12} = 2$, $k_{21} = 8$, $k_{22} = 5$, $\nu_1 = 0.05$, $\nu_2 = 0.1$, $\varrho = 1$, and $\rho = 0.45$. The updating law parameters are selected as $\Gamma_\Theta = 15 I_{64\times 64}$, $\varphi_{\bar{\delta}} = 2 I_{2\times 2}$, $\sigma_\Theta = 0.01$, and $\sigma_{\bar{\delta}} = 0.01$. The quantization parameters are set as $u_{\min} = 0.02$ and $\epsilon = 0.1$. To achieve the output constraints of the system, the constraint parameters are chosen as $c_t = 0.02$ and $\dot{c}_t = 0$.

TABLE II
System Parameter

Parameter	Value	Unit	Parameter	Value	Unit
J_f	0.0215	$\mathrm{kg \cdot m^2}$	D_d	0.0220	N/V
J_d	0.0237	$\mathrm{kg \cdot m^2}$	K_{pp}	0.0011	$\mathrm{N \cdot m/V}$
l_v	0.0025	m	K_{py}	0.0021	$\mathrm{N \cdot m/V}$
m_a	1.0750	kg	K_{yp}	−0.0027	$\mathrm{N \cdot m/V}$
D_f	0.0071	N/V	K_{yy}	0.0022	$\mathrm{N \cdot m/V}$

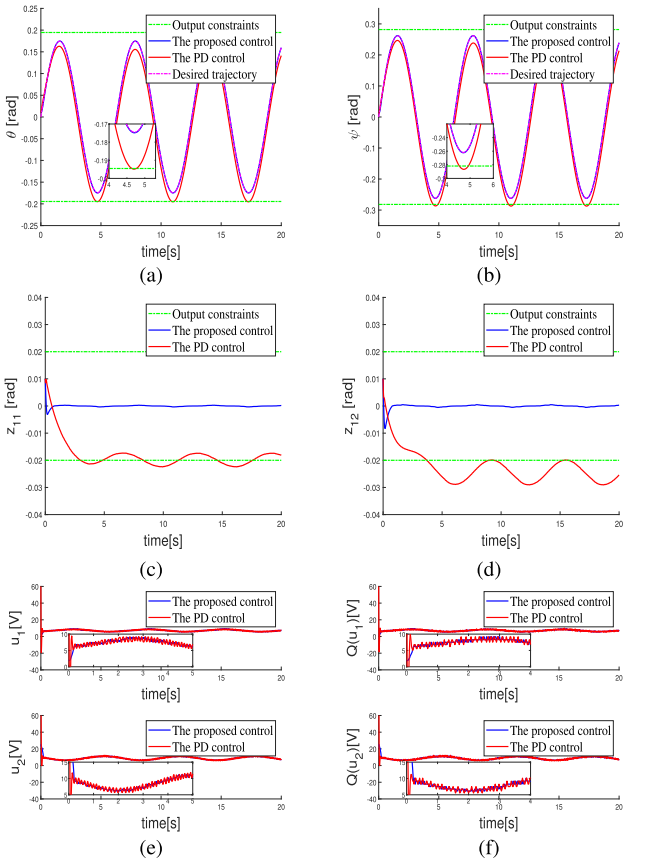

Fig. 3. Simulation results of the proposed and PD controls: (a) tracking result of θ, (b) tracking result of ψ, (c) tracking error z_{11}, (d) tracking error z_{12}, (e) control inputs u_1 and u_2, and (f) quantized inputs $Q(u_1)$ and $Q(u_2)$.

2) PD Control: We design the PD controller as

$$u_{\mathrm{PD}} = -K_p\,(q_1 - q_d) - K_d \dot{z}_1 \tag{62}$$

where K_p and K_d denote the proportional and differential gains, respectively. Through proper selection of control parameters, we choose $K_p = \mathrm{diag}[36, 36]$ and $K_d = \mathrm{diag}[40, 40]$.

The simulation results comparing the proposed and PD controls are shown in Fig. 3. Fig. 3(a) and (b) depicts the tracking performance of the pitch and yaw angles, respectively. Evidently, the proposed control method can track the desired trajectory better than the PD control, while also ensuring that the constraint boundaries are not violated. Fig. 3(c) and (d) depicts the trajectory errors of the attitude angles. The results demonstrate that the proposed method can consistently achieve smaller errors compared to the PD control and can effectively maintain the errors within the specified constraint bounds. Fig. 3(e) shows the control inputs, and Fig. 3(f) shows the quantized inputs. The proposed control strategy possesses a

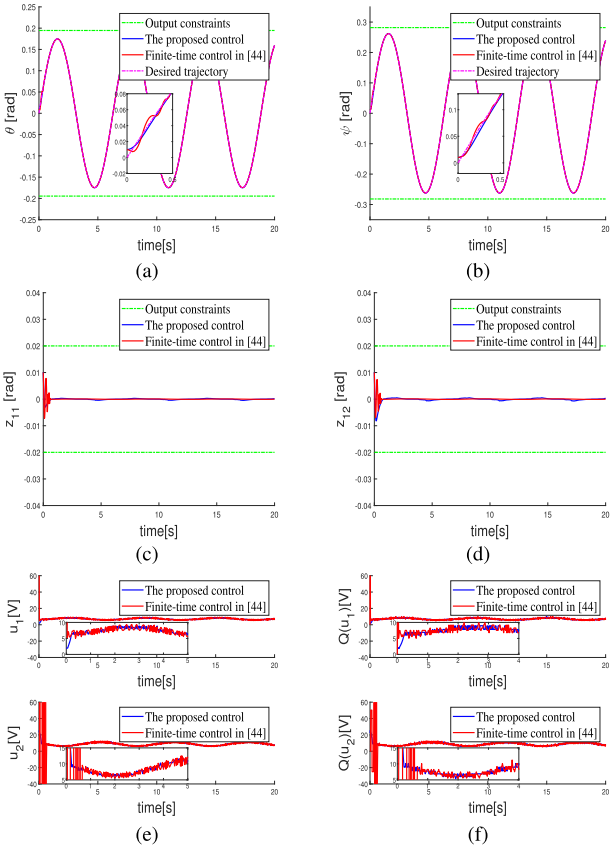

Fig. 4. Simulation results of the proposed and finite-time controls in [44]: (a) tracking result of θ, (b) tracking result of ψ, (c) tracking error z_{11}, (d) tracking error z_{12}, (e) control inputs u_1 and u_2, and (f) quantized inputs $Q(u_1)$ and $Q(u_2)$.

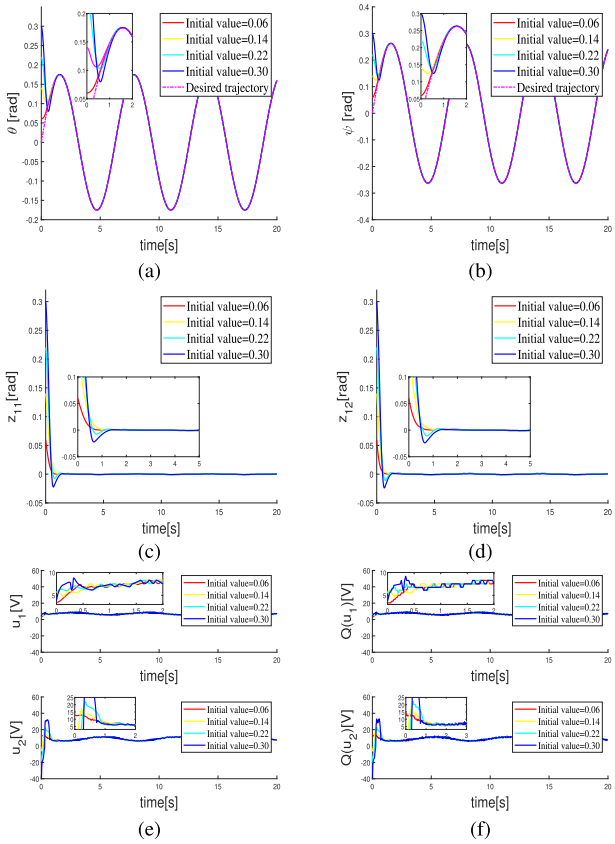

Fig. 5. Simulation results of different initial conditions: (a) tracking result of θ, (b) tracking result of ψ, (c) tracking error z_{11}, (d) tracking error z_{12}, (e) control inputs u_1 and u_2, and (f) quantized inputs $Q(u_1)$ and $Q(u_2)$.

better input response compared to PD control, as evidenced by the fact that the quantized signals exhibit reduced fluctuations.

3) Finite-Time Control in [44]: To further demonstrate the superiority of the proposed method, we also compare the adaptive finite-time neural tracking control in [44] with the proposed control. The design parameters are designed as $k_1 = k_2 = 4$.

The simulation results comparing the proposed and finite-time controls are depicted in Fig. 4. Fig. 4(a) and (b) depicts the tracking performance of the pitch and yaw angles, respectively. The results indicate that the proposed control has better tracking performance than the adaptive finite-time control. Fig. 4(c) and (d) describes the tracking errors of attitude angles. Obviously, compared to the finite-time control, the proposed method exhibits fewer oscillations at the beginning of the system. Fig. 4(e) and (f) represents the control inputs and quantized inputs, respectively. The results show that the proposed control offers superior input responses and the quantized signals have smaller fluctuations. These further validate the superiority of the proposed control.

B. Comparison of Different Initial Conditions

To verify that the convergence time of the proposed fixed-time control is independent of the initial state, we consider different values of $q = 0.06$, $q = 0.14$, $q = 0.22$, and $q = 0.30$. The control parameters are chosen as $k_{11} = 2$, $k_{12} = 2$, $k_{21} = 4$, and $k_{22} = 4$. By selecting these diverse initial conditions, we conduct a comparative analysis of the control efficacy, and the corresponding simulation results are depicted in Fig. 5. Fig. 5(a) and (b) shows the tracking responses of the attitude angles. The results show that the proposed fixed-time control exhibits good tracking performance for different initial values. The error responses are depicted in Fig. 5(c) and (d). Clearly, the tracking errors rapidly converge to a small range centered around zero in fixed time. Fig. 5(e) and (f) depicts the input voltages and quantized input signals. From the results, we can conclude that the system input can maintain excellent performance with diverse initial conditions.

Based on an analysis of the simulation data between the proposed, PD, and finite-time control methods, as well as the comparison of different initial conditions, we have validated the feasibility and superiority of the proposed control and demonstrated its superiority in terms of transient performance.

V. Experimental Results and Performance Validations

In this section, to further compare and analyze the effectiveness of the proposed control algorithm, we describe the comparative validation experiments conducted on Quanser's 2-DOF helicopter experimental platform. The experimental platform is presented in Fig. 6. Initially, the proposed control algorithm is evaluated using an experiment without output constraints. Then, the proposed strategy is compared with the finite-time control in [44] for further evaluation.

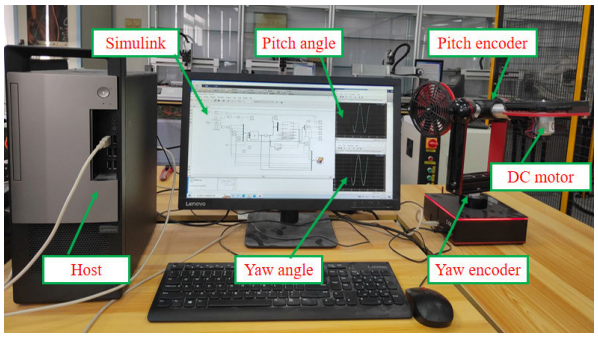

Fig. 6. Experiment platform for 2-DOF helicopter.

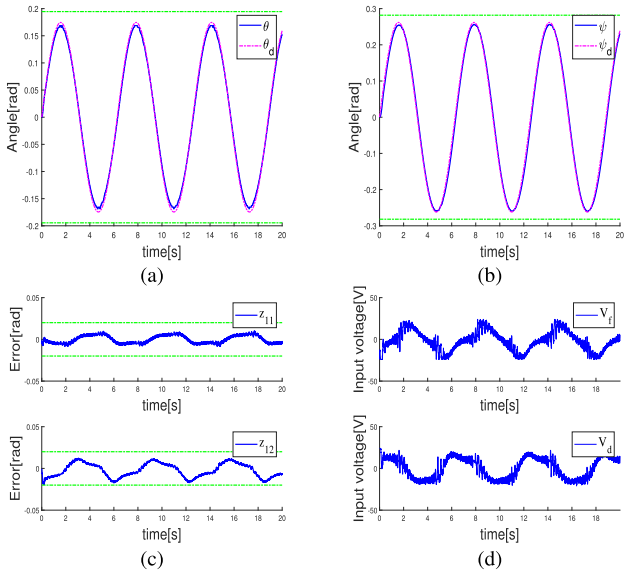

Fig. 7. Experiment results of the proposed control: (a) tracking result of θ, (b) tracking result of ψ, (c) tracking errors z_{11} and z_{12}, and (d) input voltages V_f and V_d.

We select the desired trajectory for the experiment as $q_d = [(\pi/18)\sin(t), (\pi/12)\sin(t)]^{\mathrm{T}}$, the initial conditions of the helicopter are given as $q_1 = [0, 0]^{\mathrm{T}}$ and $q_2 = [0, 0]^{\mathrm{T}}$. The control parameters are chosen as $k_{11} = 4$, $k_{12} = 4$, $k_{21} = 10$, $k_{22} = 6$. The other parameters are selected as discussed in Section IV.

A. Experiments of the Proposed Control

Fig. 7 depicts the experimental results of the proposed control. Fig. 7(a) and (b) depicts the response trajectories for the pitch and yaw angles, respectively. The figures show that both attitude angles can rapidly and accurately follow the desired trajectory. Fig. 7(c) shows that the error responses of the system remain small and consistently within the specified constrained range. Fig. 7(d) depicts the input voltages, which exhibit a favorable performance trajectory. Therefore, these results confirm that the proposed control method has excellent control performance.

B. Experiments of the Proposed Control Without Output Constraints

For further validation, we conduct an experiment without output constraints to compare with the proposed control. The experimental results are illustrated in Fig. 8. Fig. 8(a) and (b) represents the evolutions of the output angles of the system, indicating that the attitude angles effectively track the target trajectory. Fig. 8(c) depicts the errors of the system, and it reveals that without output constraints, the system errors violate the constraint range and exhibit significant oscillations. Fig. 8(d) presents the input performance. It is evident that the amplitude response of the input voltage fell short of the expected results.

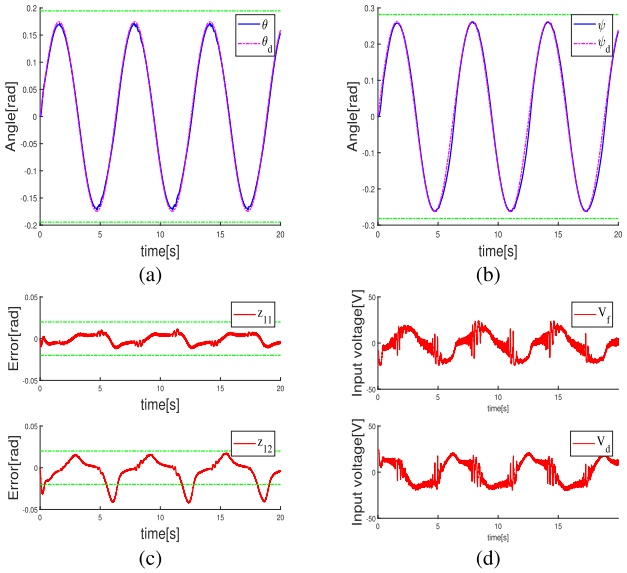

Fig. 8. Experiment results of the proposed control without output constraints: (a) tracking result of θ, (b) tracking result of ψ, (c) tracking errors z_{11} and z_{12}, and (d) input voltages V_f and V_d.

Consequently, the proposed control effectively ensures that the system errors remain within the boundaries of the output constraints. However, in the absence of output constraints, the tracking errors of the system oscillate significantly and fail to maintain errors within the acceptable limits. Moreover, the exhibited input performance is unsatisfactory.

C. Experiments of the Finite-Time Control in [44]

To further validate the superiority of the proposed control, we apply a typical finite-time-based control strategy from [44] to a 2-DOF helicopter test platform. The control parameters are chosen as $k_{11} = k_{12} = 10$. The experimental results of the finite-time control method are shown in Fig. 9. Fig. 9(a) and (b) represents the trajectory responses of the helicopter attitude angles. Fig. 9(c) depicts the trajectory errors. Fig. 9(d) represents the input voltages.

As illustrated in Fig. 9, we can observe that the finite-time control achieves tracking of the desired trajectory, with the system error evolving within the constraint range. However, by comparing the results shown in Fig. 10, we can conclude that the proposed control outperforms the finite-time control. The proposed control exhibits less volatility in the system errors, highlighting its superiority in transient performance. In addition, it demonstrates smaller input oscillations and more satisfactory performance, thus validating the effectiveness of the proposed approach.

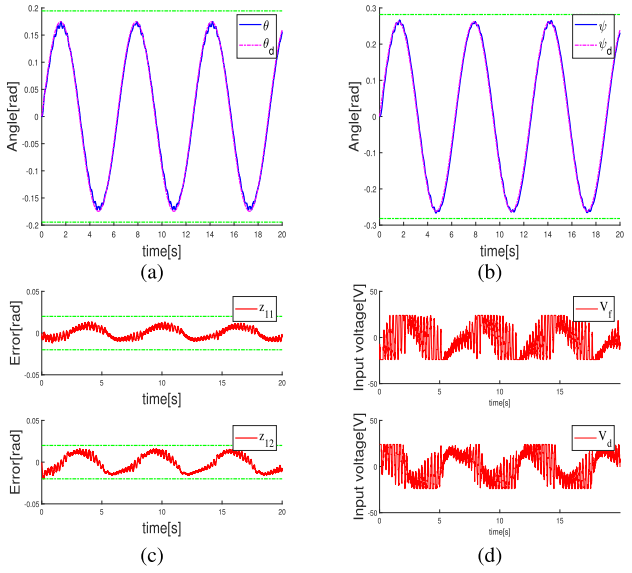

Fig. 9. Experiment results of the finite-time control in [44]: (a) tracking result of θ, (b) tracking result of ψ, (c) tracking errors z_{11} and z_{12}, and (d) input voltages V_f and V_d.

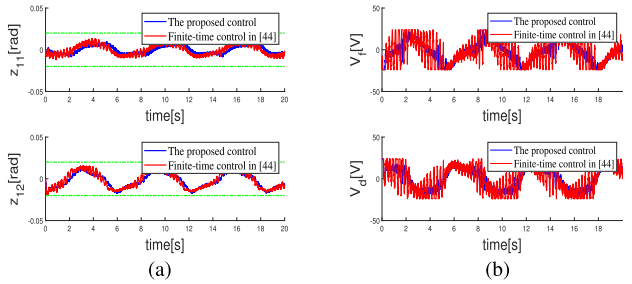

Fig. 10. Experimental comparison results between the proposed control and finite-time control: (a) comparison of errors z_{11} and z_{12} and (b) comparison of input voltages V_f and V_d.

VI. Conclusion

In this study, an NN-based adaptive fixed-time control was proposed for a 2-DOF helicopter system with input quantization and output constraints. First, a hysteresis quantizer was introduced to alleviate the chattering effect in the signal quantization process, and the error caused by the quantization was eliminated through adaptive variables. The RBFNN was then utilized to approximate the uncertainty of the system. Simultaneously, a logarithmic BLF was employed to ensure that the errors remained within the constraint range. Subsequently, through Lyapunov stability analysis and the fixed-time stability criterion, the boundedness and fixed-time convergence of the closed-loop system were guaranteed. Finally, the feasibility of the proposed control was validated through simulations and experiments. In future work, the results obtained in this study will be applied to 4-DOF drones, and the issue of output constraints occurring in a limited time interval will be explored.

References

[1] B. Ma et al., "Deep reinforcement learning of UAV tracking control under wind disturbances environments," *IEEE Trans. Instrum. Meas.*, vol. 72, pp. 1–13, 2023.

[2] Y. Yang, L. Liao, H. Yang, and S. Li, "An optimal control strategy for multi-UAVs target tracking and cooperative competition," *IEEE/CAA J. Autom. Sinica*, vol. 8, no. 12, pp. 1931–1947, Dec. 2021.

[3] Z. Zheng, J. Li, Z. Guan, and Z. Zuo, "Constrained moving path following control for UAV with robust control barrier function," *IEEE/CAA J. Autom. Sinica*, vol. 10, no. 7, pp. 1557–1570, Jul. 2023.

[4] X. Gong, M. V. Basin, Z. Feng, T. Huang, and Y. Cui, "Resilient time-varying formation-tracking of multi-UAV systems against composite attacks: A two-layered framework," *IEEE/CAA J. Autom. Sinica*, vol. 10, no. 4, pp. 969–984, Apr. 2023.

[5] M. Raghappriya and S. Kanthalakshmi, "Pitch and yaw motion control of 2 DoF helicopter subjected to faults using sliding-mode control," *Arch. Control Sci.*, vol. 32, no. 2, pp. 359–381, 2022.

[6] M. Yousfi, C. B. Njima, and T. Garna, "Decentralized nonlinear robust control for multivariable systems: Application to a 2 DoF laboratory helicopter," *Acta Polytechnica Hungarica*, vol. 17, no. 5, pp. 27–48, 2020.

[7] S. Sadala, B. Patre, and D. Ginoya, "A new continuous integral sliding mode control algorithm for inverted pendulum and 2-DOF helicopter nonlinear systems: Theory and experiment," *Proc. Inst. Mech. Eng., I, J. Syst. Control Eng.*, vol. 236, no. 3, pp. 518–530, Mar. 2022.

[8] S. Zhang, S. Yuan, X. Yu, L. Kong, Q. Li, and G. Li, "Adaptive neural network fixed-time control design for bilateral teleoperation with time delay," *IEEE Trans. Cybern.*, vol. 52, no. 9, pp. 9756–9769, Sep. 2022.

[9] G. Liu and Z. Hou, "RBFNN-based adaptive iterative learning fault-tolerant control for subway trains with actuator faults and speed constraint," *IEEE Trans. Syst. Man, Cybern. Syst.*, vol. 51, no. 9, pp. 5785–5799, Sep. 2021.

[10] M. Chen, K. Yan, and Q. Wu, "Multiapproximator-based fault-tolerant tracking control for unmanned autonomous helicopter with input saturation," *IEEE Trans. Syst. Man, Cybern. Syst.*, vol. 52, no. 9, pp. 5710–5722, Sep. 2022.

[11] Z. Zhao, W. He, F. Zhang, C. Wang, and K.-S. Hong, "Deterministic learning from adaptive neural network control for a 2-DOF helicopter system with unknown backlash and model uncertainty," *IEEE Trans. Ind. Electron.*, vol. 70, no. 9, pp. 9379–9389, Sep. 2023.

[12] C.-W. Kuo, C.-C. Tsai, and C.-T. Lee, "Intelligent leader-following consensus formation control using recurrent neural networks for small-size unmanned helicopters," *IEEE Trans. Syst. Man, Cybern. Syst.*, vol. 51, no. 2, pp. 1288–1301, Feb. 2021.

[13] G. Ma, H. Wu, Z. Zhao, T. Zou, and K. Hong, "Adaptive neural network control of a non-linear two-degree-of-freedom helicopter system with prescribed performance," *IET Control Theory Appl.*, vol. 17, no. 13, pp. 1789–1799, Sep. 2023.

[14] X. Jiang, M. Chi, X. Chen, H. Yan, and T. Huang, "Tracking and regulation performance limitations of networked control systems over erasure channel with input quantization," *IEEE Trans. Autom. Control*, vol. 67, no. 9, pp. 4862–4869, Sep. 2022.

[15] X. Zhao, S. Zhang, Z. Liu, J. Wang, and H. Gao, "Adaptive event-triggered boundary control for a flexible manipulator with input quantization," *IEEE/ASME Trans. Mechatronics*, vol. 27, no. 5, pp. 3706–3716, Oct. 2022.

[16] Z. Zhang, C. Wen, L. Xing, and Y. Song, "Adaptive output feedback control of nonlinear systems with mismatched uncertainties under input/output quantization," *IEEE Trans. Autom. Control*, vol. 67, no. 9, pp. 4801–4808, Sep. 2022.

[17] W. Wang, J. Zhou, C. Wen, and J. Long, "Adaptive backstepping control of uncertain nonlinear systems with input and state quantization," *IEEE Trans. Autom. Control*, vol. 67, no. 12, pp. 6754–6761, Dec. 2022.

[18] X. Yu, W. He, H. Li, and J. Sun, "Adaptive fuzzy full-state and output-feedback control for uncertain robots with output constraint," *IEEE Trans. Syst. Man, Cybern. Syst.*, vol. 51, no. 11, pp. 6994–7007, Nov. 2021.

[19] Z. Zhao, J. Zhang, Z. Liu, C. Mu, and K.-S. Hong, "Adaptive neural network control of an uncertain 2-DOF helicopter with unknown backlash-like hysteresis and output constraints," *IEEE Trans. Neural Netw. Learn. Syst.*, vol. 34, no. 12, pp. 10018–10027, Dec. 2023, doi: 10.1109/TNNLS.2022.3163572.

[20] L.-B. Wu, J. H. Park, X.-P. Xie, and Y.-J. Liu, "Neural network adaptive tracking control of uncertain MIMO nonlinear systems with output constraints and event-triggered inputs," *IEEE Trans. Neural Netw. Learn. Syst.*, vol. 32, no. 2, pp. 695–707, Feb. 2021.

[21] K. Li and Y. Li, "Adaptive neural network finite-time dynamic surface control for nonlinear systems," *IEEE Trans. Neural Netw. Learn. Syst.*, vol. 32, no. 12, pp. 5688–5697, Dec. 2021.

[22] S.-Y. Wei and Y.-X. Li, "Finite-time adaptive neural network command filtered controller design for nonlinear system with time-varying full-state constraints and input quantization," *Inf. Sci.*, vol. 613, pp. 871–887, Oct. 2022.

[23] C. Li, L. Zhao, and Z. Xu, "Finite-time adaptive event-triggered control for robot manipulators with output constraints," *IEEE Trans. Circuits Syst. II, Exp. Briefs*, vol. 69, no. 9, pp. 3824–3828, Sep. 2022.

[24] A. Polyakov, "Nonlinear feedback design for fixed-time stabilization of linear control systems," *IEEE Trans. Autom. Control*, vol. 57, no. 8, pp. 2106–2110, Aug. 2012.

[25] W. He, F. Kang, L. Kong, Y. Feng, G. Cheng, and C. Sun, "Vibration control of a constrained two-link flexible robotic manipulator with fixed-time convergence," *IEEE Trans. Cybern.*, vol. 52, no. 7, pp. 5973–5983, Jul. 2022.

[26] D. Zhang, S. Zhu, H. Zhang, W. Si, and W. X. Zheng, "Fixed-time consensus for multiple mechanical systems with input dead-zone and quantization under directed graphs," *IEEE Trans. Netw. Sci. Eng.*, vol. 10, no. 3, pp. 1525–1536, May 2023.

[27] Z. Zhang and Y. Wu, "Further results on fixed-time stabilization and tracking control of a marine surface ship subjected to output constraints," *IEEE Trans. Syst. Man, Cybern. Syst.*, vol. 51, no. 9, pp. 5300–5310, Sep. 2021.

[28] L. Kong, Q. Lai, Y. Ouyang, Q. Li, and S. Zhang, "Neural learning control of a robotic manipulator with finite-time convergence in the presence of unknown backlash-like hysteresis," *IEEE Trans. Syst. Man, Cybern. Syst.*, vol. 52, no. 3, pp. 1916–1927, Mar. 2022.

[29] S.-K. Kim, K. S. Kim, and C. K. Ahn, "Order reduction approach to velocity sensorless performance recovery PD-type attitude stabilizer for 2-DOF helicopter applications," *IEEE Trans. Ind. Informat.*, vol. 18, no. 10, pp. 6848–6856, Oct. 2022.

[30] S. Cui, Y. Xue, M. Lv, B. Yao, and B. Yu, "Cooperative constrained control of autonomous vehicles with nonuniform input quantization," *IEEE Trans. Veh. Technol.*, vol. 71, no. 11, pp. 11431–11442, Nov. 2022.

[31] H. Sun, L. Hou, and G. Zong, "Adaptive neural network asymptotical tracking control for an uncertain nonlinear system with input quantisation," *Int. J. Syst. Sci.*, vol. 49, no. 9, pp. 1974–1984, Jul. 2018.

[32] M. Lv, W. Yu, and S. Baldi, "The set-invariance paradigm in fuzzy adaptive DSC design of large-scale nonlinear input-constrained systems," *IEEE Trans. Syst. Man, Cybern. Syst.*, vol. 51, no. 2, pp. 1035–1045, Feb. 2021.

[33] H. Zhang and Z. Zeng, "Synchronization of nonidentical neural networks with unknown parameters and diffusion effects via robust adaptive control techniques," *IEEE Trans. Cybern.*, vol. 51, no. 2, pp. 660–672, Feb. 2021.

[34] Y. Huang, J. Wang, F. Wang, and B. He, "Event-triggered adaptive finite-time tracking control for full state constraints nonlinear systems with parameter uncertainties and given transient performance," *ISA Trans.*, vol. 108, pp. 131–143, Feb. 2021.

[35] Z. Yu, S. Li, Z. Yu, and F. Li, "Adaptive neural output feedback control for nonstrict-feedback stochastic nonlinear systems with unknown backlash-like hysteresis and unknown control directions," *IEEE Trans. Neural Netw. Learn. Syst.*, vol. 29, no. 4, pp. 1147–1160, Apr. 2018.

[36] H. Yang and J. Liu, "An adaptive RBF neural network control method for a class of nonlinear systems," *IEEE/CAA J. Autom. Sinica*, vol. 5, no. 2, pp. 457–462, Mar. 2018.

[37] J. Ni and P. Shi, "Global predefined time and accuracy adaptive neural network control for uncertain strict-feedback systems with output constraint and dead zone," *IEEE Trans. Syst. Man, Cybern. Syst.*, vol. 51, no. 12, pp. 7903–7918, Dec. 2021.

[38] W. Sun, S. Diao, S.-F. Su, and Z.-Y. Sun, "Fixed-time adaptive neural network control for nonlinear systems with input saturation," *IEEE Trans. Neural Netw. Learn. Syst.*, vol. 34, no. 4, pp. 1911–1920, Apr. 2023.

[39] X. Zhang, J. Tan, J. Wu, and W. Chen, "Event-triggered-based fixed-time adaptive neural fault-tolerant control for stochastic nonlinear systems under actuator and sensor faults," *Nonlinear Dyn.*, vol. 108, no. 3, pp. 2279–2296, May 2022.

[40] L. Li, Z. Liu, S. Guo, Z. Ma, and P. Huang, "Adaptive practical predefined-time control for uncertain teleoperation systems with input saturation and output error constraints," *IEEE Trans. Ind. Electron.*, vol. 71, no. 2, pp. 1842–1852, Feb. 2024, doi: 10.1109/TIE.2023.3250752.

[41] S. Liu, B. Jiang, Z. Mao, and Y. Zhang, "Neural-network-based adaptive fault-tolerant cooperative control of heterogeneous multiagent systems with multiple faults and DoS attacks," *IEEE Trans. Neural Netw. Learn. Syst.*, vol. 35, no. 5, pp. 6273–6285, May 2023, doi: 10.1109/TNNLS.2023.3282234.

[42] C. He, J. Wu, J. Dai, Z. Zhe, and T. Tong, "Fixed-time adaptive neural tracking control for a class of uncertain nonlinear pure-feedback systems," *IEEE Access*, vol. 8, pp. 28867–28879, 2020.

[43] W. Yang, Y. Pan, and H. Liang, "Event-triggered adaptive fixed-time NN control for constrained nonstrict-feedback nonlinear systems with prescribed performance," *Neurocomputing*, vol. 422, pp. 332–344, Jan. 2021.

[44] H. Wang, S. Liu, and W. Bai, "Adaptive neural tracking control for non-affine nonlinear systems with finite-time output constraint," *Neurocomputing*, vol. 397, pp. 60–69, Jul. 2020.

Zhijia Zhao (Member, IEEE) received the B.Eng. degree in automatic control from the North China University of Water Resources and Electric Power, Zhengzhou, China, in 2010, and the M.Eng. and Ph.D. degrees in automatic control from the South China University of Technology, Guangzhou, China, in 2013 and 2017, respectively.

He is currently a Professor with the School of Mechanical and Electrical Engineering, Guangzhou University, Guangzhou. His research interests include adaptive and learning control, flexible mechanical systems, and robotics.

Jiale Wu received the B.Eng. degree from Guangdong Ocean University, Zhanjiang, China, in 2021. He is currently pursuing the master's degree with the School of Mechanical and Electrical Engineering, Guangzhou University, Guangzhou, China.

His research interests include adaptive control, intelligent control, and robotics.

Chaoxu Mu (Senior Member, IEEE) received the Ph.D. degree in control science and engineering from the School of Automation, Southeast University, Nanjing, China, in 2012.

She was a Visiting Ph.D. Student with the Royal Melbourne Institute of Technology University, Melbourne, VIC, Australia, from 2010 to 2011. She was a Post-Doctoral Fellow with the Department of Electrical, Computer and Biomedical Engineering, The University of Rhode Island, Kingston, RI, USA, from 2014 to 2016. She is currently a Professor with the School of Electrical and Information Engineering, Tianjin University, Tianjin, China. She has authored more than 100 journal articles and conference papers and coauthored two monographs. Her current research interests include nonlinear system control and optimization and adaptive and learning systems.

Yu Liu (Senior Member, IEEE) received the Ph.D. degree in automatic control from the South China University of Technology, Guangzhou, China, in 2009.

He was a Visiting Student with the Department of Mechanical Engineering, Concordia University, Montreal, QC, Canada, from 2008 to 2009, and a Visiting Scholar with the Department of Electrical and Computer Engineering, University of Nebraska–Lincoln, Lincoln, NE, USA, from 2017 to 2018. He is currently a Professor with the School of Automation Science and Engineering, South China University of Technology, with the Research and Development Center of Precision Electronic Manufacturing Technology, Guangzhou Institute of Modern Industrial Technology, Guangzhou, and with the High Performance Motor and Intelligent Control Engineering Technology Research Center of Guangdong Province, Shenzhen, China. His current research interests include distributed parameter systems, robot control, intelligent control, intelligent perception and decision-making, and machine vision.

Dr. Liu is currently an Associate Editor of IEEE TRANSACTIONS ON NEURAL NETWORKS AND LEARNING SYSTEMS, IEEE TRANSACTIONS ON FUZZY SYSTEMS, and IEEE TRANSACTIONS ON COMPUTATIONAL SOCIAL SYSTEMS.

Keum-Shik Hong (Fellow, IEEE) received the B.S. degree in mechanical design from Seoul National University, Seoul, South Korea, in 1979, the M.S. degree in mechanical engineering from Columbia University, New York City, NY, USA, in 1987, and the M.S. degree in applied mathematics and the Ph.D. degree in mechanical engineering from the University of Illinois at Urbana–Champaign, Champaign, IL, USA, in 1991.

He joined the School of Mechanical Engineering, Pusan National University, Busan, South Korea, in 1993. His research interests include brain–computer interface, nonlinear systems theory, adaptive control, and distributed parameter systems.

Dr. Hong is a fellow of the Korean Academy of Science and Technology, an ICROS Fellow, and a member of the National Academy of Engineering of Korea. He was a past President of the Institute of Control, Robotics and Systems (ICROS), South Korea, and is the President of the Asian Control Association. He received many awards, including the Best Paper Award from the KFSTS of Korea in 1999 and the Presidential Award of Korea in 2007. He served as an Associate Editor for *Automatica* (2000–2006) and the Editor-in-Chief for *Journal of Mechanical Science and Technology* (2008–2011). He is serving as the Editor-in-Chief for *International Journal of Control, Automation, and Systems*.